Determination of the phonon dispersion of zinc blende $(3\mathrm{C})$ silicon carbide by inelastic x-ray scattering ⊘

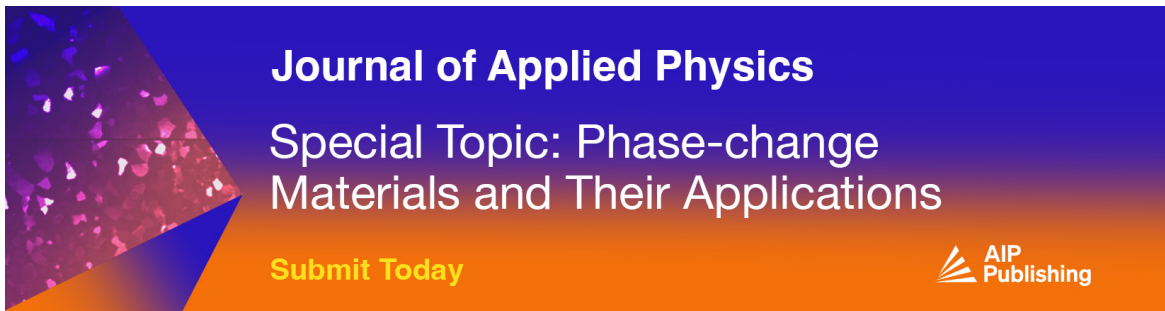J. Serrano; J. Strempfer; M. Cardona; M. Schwoerer-Böhning; H. Requardt; M. Lorenzen; B. Stojetz; P. Pavone; W. J. Choyke

Check for updates

CrossMark

View Online

Export Citation

Determination of the phonon dispersion of zinc blende (3*C*) silicon carbide by inelastic x-ray scattering

J. Serrano,[a] J. Strempfer, and M. Cardona
Max-Planck-Institut für Festkörperforschung, Heisenbergstrasse 1, 70569 Stuttgart, Germany

M. Schwoerer-Böhning
Advanced Photon Source (APS), Argonne National Laboratory, Argonne, Illinois 60439-4814

H. Requardt and M. Lorenzen
European Synchrotron Radiation Facility (ESRF), Boîte Postale 220, 38043 Grenoble, France

B. Stojetz and P. Pavone
Institut für Theoretische Physik, Universität Regensburg, 93040 Regensburg, Germany

W. J. Choyke
Department of Physics, University of Pittsburgh, Pittsburgh, Pennsylvania 15260

We present an experimental and theoretical investigation of the phonon dispersion relations in zinc blende (3*C*) SiC. The experimental data were obtained for the entire Brillouin zone by inelastic x-ray scattering (IXS) using a synchrotron radiation source. Eigenvector analysis is performed with the aid of state-of-the-art linear response first principles calculations based on density functional theory. The theoretical predictions reproduce the experimental phonon dispersion remarkably well. These results are compared with data obtained previously for the $\langle 111 \rangle$ direction by Raman spectroscopy using several SiC polytypes and the backfolding technique. IXS data for 4*H* modification along the *c* axis are also reported. © *2002 American Institute of Physics.* [DOI: 10.1063/1.1484241]

Wide band gap materials have attracted considerable attention because of their potential for the fabrication of optoelectronic devices and for high-power, high-temperature applications. Silicon carbide has generated interest not only because of its large band gap, but also because of its large thermal conductivity, high breakdown voltage, and outstanding mechanical and chemical stability. A major concern with this semiconductor is the large number of polytypes in which it crystallizes[1] and the difficulties in growing single-polytype crystals.

In spite of the wealth of information available on the electronic and optical properties of SiC, the phonon dispersion relations have not yet been experimentally determined (except[2] for 6*H*-SiC). Knowledge of the phonon dispersion in the entire Brillouin zone (BZ) is an indispensable step for further investigation of interesting properties such as phonon-assisted photoemission, thermal expansion, and thermal conductivity. Moreover, phonons can influence the behavior of carriers in devices through electron–phonon interaction. The scant amount of experimental information available concerns mainly the $\Gamma-L$ direction of zinc blende (3*C*) SiC, and it has been indirectly obtained by means of Raman spectroscopy of several polytypes,[3–5] using the conjecture that the phonon dispersion along the $\Gamma-A$ direction in hexagonal modifications can be backfolded onto the $\Gamma-L$ direction of the zinc blende structure.[3] However, the lattice dynamics of SiC polytypes have been studied with several theoretical models.[6,7] Experimental determination of

the phonon dispersion in 3*C*-SiC can also be used to describe the subtle variations in the phonon dispersion of other hexagonal polytypes that arises from the different stacking order along the *c* axis. Empirical information on the eigenvectors has been reported only for the $\langle 111 \rangle$ direction.[5] This work was performed by Raman spectroscopy using several polytypes grown with different silicon isotopes. Eigenvectors provide a more exhaustive way of testing lattice dynamical models, but unfortunately experimental data on eigenvectors are very scarce.

The lack of sizeable samples and the high frequency of the optical modes of SiC hamper direct investigation of the phonon dispersion relations by inelastic neutron scattering (INS). With the advent of highly brilliant third-generation synchrotron radiation sources it has become possible to circumvent this issue by the use of inelastic x-ray scattering (IXS). With this technique, determination of phonon dispersions in crystals of millimeter size has become a routine task (see Refs. 8–10 for data on diamond, AlN, and GaN, respectively).

In this letter we report room temperature measurements of the phonon dispersion relations for 3*C*-SiC in the entire BZ obtained by inelastic x-ray scattering. We compare the 3*C*-SiC IXS data with those previously obtained by Raman spectroscopy of polytypes and with IXS data, also shown here, for 4*H*-SiC along the $\Gamma-A$ direction. *Ab initio* linear response calculations of phonon dispersion based on density functional theory (DFT) which were used during the experiments as a guide to determine the optimal scattering geometries are also presented. Excellent agreement is found between the calculations and the experimental data, not only

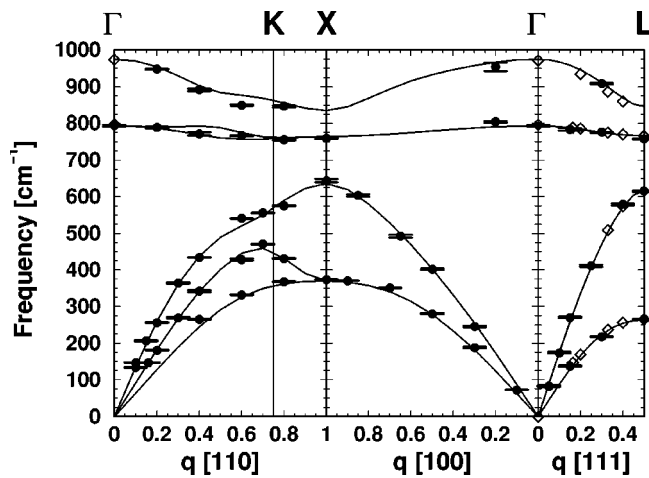[a]Electronic mail: j.serrano@fkf.mpg.de

FIG. 1. Phonon dispersion relations of 3*C*-SiC. IXS data (closed circles) are displayed together with *ab initio* phonon dispersion (solid lines) and Raman data (open diamonds) from Ref. 5. The *x* axes are scaled in reciprocal lattice units.

for the phonon frequencies but also for the eigenvectors investigated. Our results are compared with INS data[2] for 6*H*-SiC.

Measurements on 3*C*-SiC (4*H*-SiC) were performed on a $5 \times 2 \times 1.5$ mm^3 ($4 \times 5 \times 0.8$ mm^3) sample with its surface oriented perpendicular to the [111] direction (*c* axis). The widths of rocking scans across Bragg reflections were around 0.015° and 0.014° for cubic and hexagonal polytypes, respectively.

IXS experiments were carried out at the European Synchrotron Radiation Facility (ESRF) in Grenoble (beam line ID28). The energy of the incident radiation (17.794 keV) was defined by the silicon (999) Bragg reflection order at the monochromator, and yielded instrumental energy resolution of ≈ 20 cm^{-1} and momentum resolution of ≈ 0.28 nm^{-1}. Both, wave vector and energy scans were performed, the latter by varying the difference in temperature between the monochromator and the analyzer. Details of the instrument can be found elsewhere.[10,11] With this configuration, phonon frequencies were determined to within ± 2 cm^{-1}. Effects of possible temperature drifts of the monochromator–analyzer system for the energy scans, which could lead to variations in the zero-energy offset, were largely eliminated by performing systematic Stokes-anti-Stokes scans.

The *ab initio* calculations for 3*C*-SiC used in this experiment are similar to those reported in Ref. 7. We utilized the formalism of density functional perturbation theory within the local-density approximation. A basis set of plane waves with a kinetic-energy cutoff of 70 (50) Ry was considered for converged calculations of the structural (dynamical) properties. We employed nonlocal pseudopotentials[12] for description of the electron–ion interaction as well as a mesh of 10 special points for Brillouin-zone integration. Minimization of the total energy with respect to the lattice constant yields a value of $a_{3C} = 4.308$ Å for the zinc blende structure. This value is in good agreement with the one obtained experimentally from several Bragg reflections $a_{3C} = 4.360(2)$ Å. For the cubic structure, dynamical matrices were calculated for a regular mesh in reciprocal space and interatomic force constants (IFCs) in real space were ex-

tracted from them by Fourier transformation. This procedure enabled the calculation of frequencies and eigenvectors of 3*C*-SiC from the IFCs at arbitrary points in reciprocal space. For hexagonal 4*H*-SiC a different procedure was used. The IFCs of 4*H*-SiC were obtained from those calculated for 3*C*-SiC and 2*H*-SiC by a procedure of local-coupling transfer[13] in which we used explicitly the similarity between the local structure of the different polytypes.

Figure 1 shows the phonon frequencies measured for 3*C*-SiC (closed circles) together with those calculated (solid lines). The open diamonds correspond to Raman data[5] for 6*H*- and 15*R*-SiC. There is good agreement between the IXS data and the *ab initio* results, with deviation less than 3%. The error bars correspond to the sum of the error of the fit plus fluctuations in the monochromator calibration. A lower intensity of the signal was observed for optic modes. Eigenvector analysis of the IXS data allows the assignment of the longitudinal and transverse character of the different phonon branches. This is especially important along the Γ-*K*-*X* direction, where, e.g., the phonon frequencies measured for the transverse optic (TO) modes correspond to those of the lower branch, in agreement with the calculation.

In Table I we summarize the phonon frequencies of the main high symmetry points of the BZ, and compare them with the calculation and, for the Γ and *L* points, with Raman data[5] obtained from several polytypes. Low temperature photoluminescence (LTPL) measurements performed on the same 3*C*-SiC sample yielded data for phonons at the *X* point
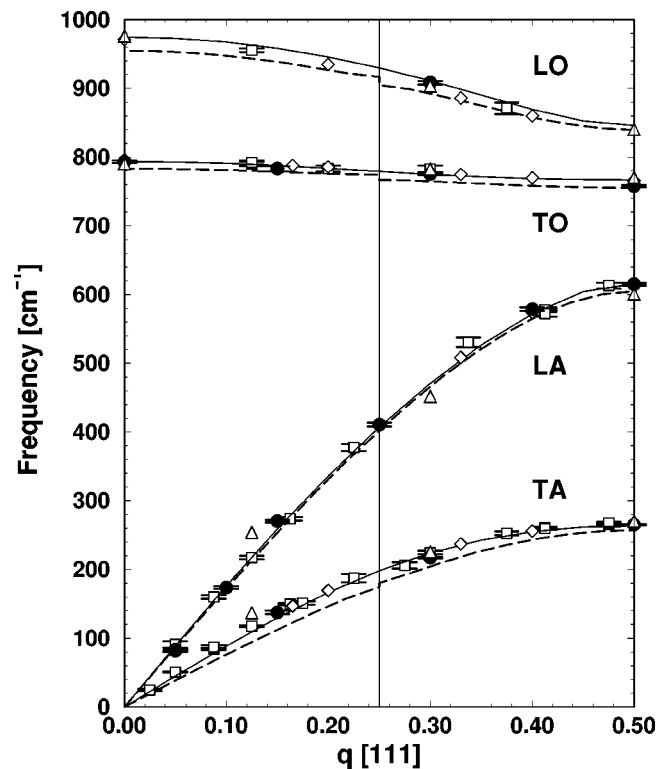

FIG. 2. Comparison between 3*C*- (closed circles) and 4*H*-SiC (open squares) IXS data of the phonon frequencies along the *c* axis and the ⟨111⟩ direction, respectively. Open diamonds correspond to Raman data (see Ref. 5) obtained from other polytypes using the backfolding technique. Open triangles represent INS data for 6*H*-SiC reported in Ref. 2. Solid lines and dashed lines show the dispersion calculated for 3*C*- and 4*H*-SiC, respectively. Note the discontinuities in the latter at $q=0.25$ [111] that arise from different stacking of the planes along the *c* axis.

TABLE I. Frequencies of several high-symmetry phonons in $3C$-SiC determined by inelastic x-ray scattering, compared with experimental data from Raman spectroscopy and photoluminescence and theoretical data. The transverse-longitudinal and acoustic-optic characters of the phonons are specified as well (e.g., LO stands for the longitudinal optical character). Nonequivalent tranverse phonons at the K point are indexed ordered according to increasing frequency.

Symmetry point	Mode type	IXS[a]	Other experiments	Theory[b]
Γ	TO	793(2)	796(1)[c]	793.1
Γ	LO		971(1)[c]	974.8
K	TA_1	368(1)[d]		355.7[d]
K	TA_2	450(2)[d]		445.3[d]
K	LA	565(2)[d]		569.3[d]
K	TO_1	758(2)[d]		758.4[d]
K	TO_2			762.1[d]
K	LO	849(3)[d]		862.0[d]
X	TA	373(1)	372.6[e]	370.2
X	LA	644(6)	639.6[e]	635.1
X	TO	759(2)	763.0[e]	763.8
X	LO		829.9[e]	834.4
L	TA	265(1)	265(1)[f]	263.6
L	LA	615(2)		615.9
L	TO	758(2)	766(1)[f]	767.1
L	LO			845.6

[a]300 K data.
[b]0 K calculation.
[c]300 K Raman data from Ref. 5.
[d]Interpolated from values at $q=0.7$ [1 1 0] and -0.8 [1 1 0] in reciprocal lattice units.
[e]2 K LTPL data.
[f]300 K Raman data obtained from a $6H$-SiC polytype (Ref. 5).

in good agreement with those obtained by IXS.

In Fig. 2 we show IXS data for $3C$-SiC along the Γ-L direction (closed circles) together with those obtained for the $4H$-SiC (open squares) and Raman data[5] from other hexagonal and rombohedral polytypes (open diamonds), along the $\langle 001 \rangle$ direction, backfolded onto the $3C$-SiC dispersion.[3] Open triangles display INS data on $6H$-SiC from Ref. 2. Despite the different stacking planes along the c axis, which can be realized in the calculated results at $q=0.25$ [111], there is a clear overlap of the experimental data of hexagonal, rhombohedral, and cubic polytypes. The accuracy of the calculations does not allow us to establish a clear difference between data for $3C$ and those for other polytypes, although compared to the IXS data, the calculation underestimates the frequencies of the transverse acoustic (TA) phonons for the $4H$ modification. These systematic deviations are probably related to the use of the local-coupling transfer approximation for the IFC of $4H$-SiC.[13] For the transverse optic phonons, a slightly lower frequency is found for $3C$-SiC

than for the other polytypes. This difference among polytypes could arise from the different second neighbor arrangement. Calculated results for phonon eigenvectors correlate well with those reported in Ref. 5, e.g., for $q=0.4$ [111]$2\pi/a_{3C}$ we obtained $(e_{Si}, e_C) = (0.947, 0.321)$ for the longitudinal acoustic (LA) modes and the experimental data by Raman spectroscopy in several polytypes are (0.948, 0.318).

In conclusion, we have reported data for the phonon dispersion relations of $3C$- and $4H$-SiC obtained by inelastic x-ray scattering, analyzed with the aid of first-principles calculations. Good agreement was found between theory and experiment, both in the phonon frequencies and eigenvectors. The comparison of $3C$- and $4H$-SiC phonon frequencies along the $\langle 111 \rangle$ and $\langle 001 \rangle$ directions, respectively, confirms the validity of the backfolding technique used in the past to model the phonon dispersion along those directions. A more comprehensive study of the phonon dispersion of $4H$-SiC along other directions will be presented elsewhere.[14]

[1] *Silicon Carbide. A Review of Fundamental Questions and Applications to Current Device Technology*, edited by W. J. Choyke, H. Matsunami, and G. Pensl (Akademie, Berlin, 1998), Vols. I and II.
[2] B. Dorner, H. Schober, A. Wonhas, M. Schmitt, and D. Strauch, Eur. Phys. J. B **5**, 839 (1998).
[3] D. W. Feldman, J. H. Parker, Jr., W. J. Choyke, and L. Patrick, Phys. Rev. **173**, 787 (1968).
[4] S. Nakashima and H. Harima, Phys. Status Solidi A **162**, 39 (1997).
[5] F. Widulle, T. Ruf, O. Buresch, A. Debernardi, and M. Cardona, Phys. Rev. Lett. **82**, 3089 (1999).
[6] M. Hofmann, A. Zywietz, K. Karch, and F. Bechstedt, Phys. Rev. B **50**, 13401 (1994).
[7] K. Karch, P. Pavone, W. Windl, O. Schütt, and D. Strauch, Phys. Rev. B **50**, 17054 (1994).
[8] M. Schwoerer-Böhning, A. T. Macrander, and D. A. Arms, Phys. Rev. Lett. **80**, 5572 (1998).
[9] M. Schwoerer-Böhning, A. T. Macrander, M. Papst, and P. Pavone, Phys. Status Solidi B **215**, 177 (1999).
[10] T. Ruf, J. Serrano, M. Cardona, P. Pavone, M. Pabst, M. Krisch, M. D'Astuto, T. Suski, I. Grzegory, and M. Leszczynski, Phys. Rev. Lett. **86**, 906 (2001).
[11] C. Masciovecchio, U. Bergmann, M. Krisch, G. Ruocco, F. Sette, and R. Verbeni, Nucl. Instrum. Methods Phys. Res. B **111**, 181 (1996); **117**, 339 (1996).
[12] N. Troullier and J. L. Martins, Phys. Rev. B **43**, 1993 (1991).
[13] B. Stojetz (unpublished).
[14] J. Serrano (unpublished).